

High Performance Millimeter Wave SIW Slotted Array Antenna

Kunooru Bharath*, Srujana V. Nandigama,
Rama K. Dasari, and Vijay M. Pandharipande

Abstract—A high performance substrate integrated waveguide (SIW) slotted array antenna with low sidelobe level and optimum gain at 28 GHz is designed, and experimental results are presented with simulated data. In order to achieve a low sidelobe level, Chebyshev power coefficients in the form of slot displacements are applied to the SIW array antenna. A MATLAB program has been written to find these slot displacements. This work entails investigating and designing the optimum microstrip to SIW transition over the Ka-band, designing a 1×8 slotted SIW array antenna, and finally applying the Chebyshev power coefficients to the slots of the 1×8 SIW array antenna. The fabricated prototype of a 1×8 SIW slotted array antenna is tested, and its performance is studied in terms of gain and half power beam width (HPBW), compared with simulations. The measured results of the 1×8 slotted SIW array antenna at 28 GHz have a $|S_{11}|$ of better than -20 dB, a gain of 13 dB, and an HPBW of 17° . The overall dimensions of the design at 28 GHz are $7.143 \text{ mm} \times 51.8 \text{ mm} \times 0.254 \text{ mm}$ ($0.667\lambda_o \times 4.84\lambda_o \times 0.023\lambda_o = 0.0766\lambda_o^3 \text{ mm}^3$).

1. INTRODUCTION

Low sidelobe level (SLL) millimeter-wave (mm-wave) antennas are preferred in radar and future wireless communications to reduce interference from jamming environments. However, due to surface wave effects and mutual coupling of radiating elements, realising arrays with low SLL is difficult for planar array antennas [1]. Substrate integrated waveguide (SIW) technology has been proposed as a viable alternative at microwave and mm-wave frequencies.

SIW is a planar version of a rectangular waveguide [2], in which only TE_{m0} modes exist. Compact size, low power losses, efficient power handling, and integration capabilities are a few of its advantages. By different methods, such as method of lines (MoL) [3], numerical multimode calibration (NMC) [4], finite-difference frequency-domain (FDFD) [5], and the boundary integral-resonant mode expansion (BI-RME) [6], the propagation characteristics of rectangular waveguide and SIW are the same. In papers [7, 8], the authors discuss transitions such as coplanar waveguide to SIW, microstrip to SIW, and a simple taper that converts quasi-TEM to TE_{m0} mode. SIW slotted array antennas have gained much attention for their high efficiency, high gain, low SLLs, and low cross polarisation characteristics [9].

Several low SLL slotted waveguide and slotted SIW arrays are proposed in the literature. Elliott proposed two equations based on Stevenson's theory [10], and these equations are used to find the length and displacement of each slot in the rectangular waveguide [11]. El Misilmani et al. carried out an investigation into waveguide based slotted array antennas with low SLL at 10 GHz using different distribution techniques [12]. Dewantari et al. proposed a new technique to reduce the SLL in a slotted SIW array at 94 GHz. In this technique, amplitude tapering is achieved by changing the SIW width without altering the slot length [13]. An SLL of -20 dB is achieved in a coplanar waveguide (CPW) fed slotted SIW array antenna using Taylor distribution in [14], and to get a -30 dB SLL, the Taylor

Received 25 July 2022, Accepted 1 September 2022, Scheduled 3 October 2022

* Corresponding author: Kunooru Bharath (bharath35@osmania.ac.in).

The authors are with the Centre for Excellence in Microwave Engineering, Osmania University, Hyderabad, India.

continuous root matching sampling distribution technique is used in the SIW array at 10 GHz [15]. To achieve low SLL performance, Taylor distribution with a phase-balanced SIW feeding structure was designed at 28 GHz [16]. In [17], low SLL is achieved by adjusting the two slots in the centre of the SIW array.

This work focuses on designing a high performance SIW slotted array antenna at 28 GHz with low sidelobe level and optimum gain. To achieve this, Chebyshev power coefficients in the form of slot displacements are applied to the slots of the 1×8 SIW array antenna. In the design process, initially a microstrip to SIW transition at Ka-band is designed, then based on Elliott's procedure [11] and the procedure in [12], approximate design equations for the slot length, width, and offsets of the slotted SIW array are written to achieve low SLL. The Chebyshev power coefficients depend on the slot displacement positions. The slot displacements for the desired SLL were calculated by solving these equations using MATLAB. By using these calculated slot displacements, the 1×8 slotted SIW array has been designed and optimized in Ansys HFSS. Then, a prototype of the SIW array has been fabricated and tested. The presented 1×8 slotted SIW array has low sidelobe level and good gain with low cross polarization. Its overall size is less ($0.667\lambda_o \times 4.84\lambda_o \times 0.023\lambda_o = 0.0766\lambda_o^3 \text{ mm}^3$) than the existing designs in literature.

2. MICROSTRIP TO SIW TRANSITION DESIGN

The microstrip taper portion, as shown in Fig. 1(a), serves as a transition from the microstrip line to SIW. In this transition, the quasi-TEM mode of the microstrip line is converted to the SIW TE_{10} mode. The (p) pitch (distance between two cylindrical vias), (a_{SIW}) the distance between the two rows of cylindrical vias, and (d) the diameter of the cylindrical via are calculated by using Equations (1) & (2). According to the formulae outlined in [7, 8] and using Equations (3) to (5), the microstrip line length (L_{ml}) and width (w_{ml}) can be calculated, whereas the taper width (w_t) can be calculated from Equations (6) to (8). The SIW and taper calculated dimensions are displayed in Table 1. This structure is modelled on 10 mil thick (RT duroid-5880) substrate with 2.2 dielectric constant. Fig. 1(b) shows that the measured insertion loss is better than 0.6 dB, and the reflection parameter is better than 10 dB over the Ka-band which are in good agreement with the simulated data. Ansys HFSS 3D electromagnetic

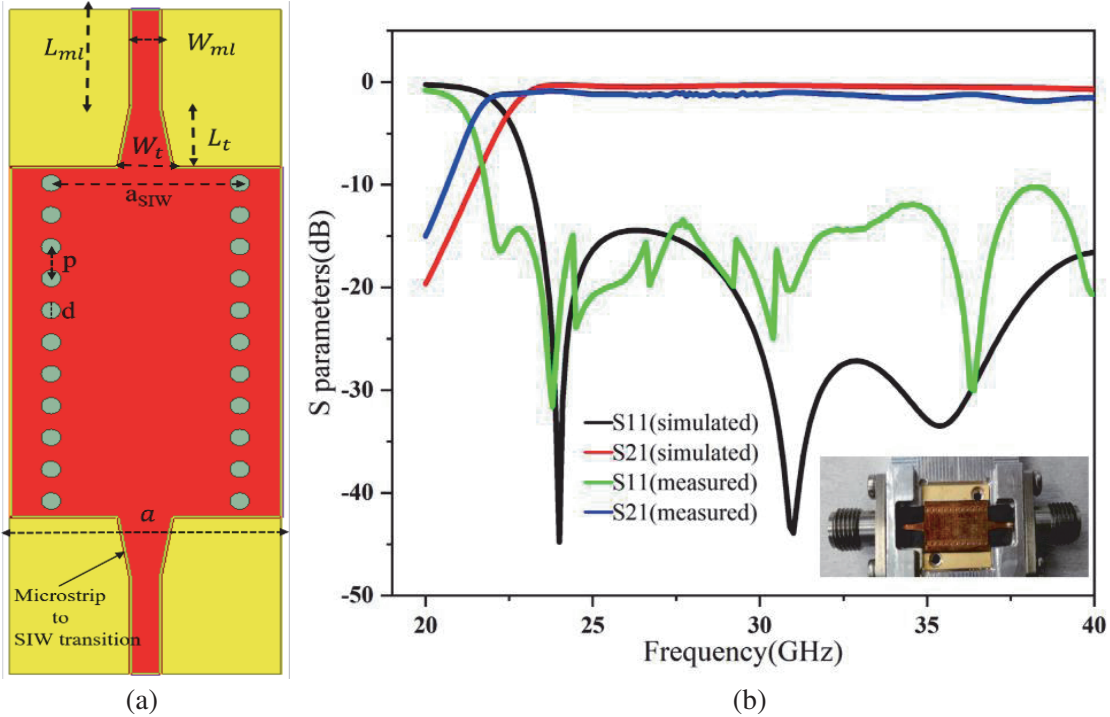


Figure 1. Microstrip to SIW structure. (a) Design top view. (b) S -parameters.

Table 1. Dimensions of the transition structure.

Parameter	W_{ml}	L_{ml}	W_t	L_t	a_{SIW}	p	d	a
Value (mm)	0.78	3	1.45	1.91	4.97	0.99	0.51	7.143

software is used to model the slotted SIW array antenna and other required designs.

$$a_{SIW} = \frac{a}{\sqrt{\varepsilon_r}} + \frac{d^2}{0.95p} \quad (1)$$

where

$$d < \frac{\lambda_g}{5} \quad \text{and} \quad p < 2d$$

$$\lambda_g = \frac{2\pi}{\sqrt{\varepsilon_r \left(\left(\frac{2\pi f_0}{c} \right)^2 - \left(\frac{\pi}{a} \right)^2}} \quad (2)$$

Here λ_g is the guided wavelength.

$$\frac{w_{ml}}{h} = \frac{8e^A}{e^{2A} - 2} \quad \text{for} \quad \frac{w_{ml}}{h} < 2 \quad (3)$$

$$w_{ml} = \frac{2h}{\pi} \left[B - 1 - \ln(2B - 1) + \frac{\varepsilon_r + 1}{2\varepsilon_r} \left\{ \ln(B - 1) + 0.39 - \left(\frac{0.61}{\varepsilon_r} \right) \right\} \right] \quad \text{for} \quad \frac{w_{ml}}{h} > 2 \quad (4)$$

where

$$A = \frac{Z_0}{60} \left(\frac{\varepsilon_r + 1}{2} \right)^{0.5} + \left[(\varepsilon_r - 1)(\varepsilon_r + 1) \left(0.23 + \frac{0.11}{\varepsilon_r} \right) \right]$$

$$B = \frac{377\pi}{2Z_0\sqrt{\varepsilon_r}}$$

$$\theta = \sqrt{\varepsilon_{eff}} k_0 L_{ml} \quad (5)$$

where

$$\varepsilon_{eff} = \frac{\varepsilon_r + 1}{2} + \left(\frac{\varepsilon_r - 1}{2} \right) \left(1 + \frac{12h}{w_{ml}} \right)^{-\frac{1}{2}}$$

A microstrip line's waveguide modal impedance is given by

$$Z_e = \sqrt{\frac{\mu}{\varepsilon_0 \varepsilon_e} \frac{h}{w_t}} = \left\{ \begin{array}{l} \frac{60}{\sqrt{\varepsilon_e}} \ln \left(\frac{8h}{w_{ml}} + \frac{0.25h}{w_{ml}} \right) \quad \text{for} \quad \frac{w_{ml}}{h} < 1 \\ \frac{120\pi}{\sqrt{\varepsilon_e} \left(\frac{w_{ml}}{h} + 1.393 + 0.667 \ln \left(\frac{w_{ml}}{h} + 1.444 \right) \right)} \quad \text{for} \quad \frac{w_{ml}}{h} > 1 \end{array} \right\} \quad (6)$$

where

$$\frac{a_{siw}}{w_t} = 4.38 e^{\frac{-0.627\varepsilon_r}{\varepsilon_e}} \quad (7)$$

Combining and rewriting the above equations, we get:

$$\frac{1}{w_t} = \left\{ \begin{array}{l} \frac{60}{\eta h} \ln \left(\frac{8h}{w_{ml}} + \frac{0.25h}{w_{ml}} \right) \quad \text{for} \quad \frac{w_{ml}}{h} < 1 \\ \frac{120\pi}{\eta h \left(\frac{w_{ml}}{h} + 1.393 + 0.667 \ln \left(\frac{w_{ml}}{h} + 1.444 \right) \right)} \quad \text{for} \quad \frac{w_{ml}}{h} > 1 \end{array} \right\} \quad (8)$$

$$\frac{1}{w_t} = \frac{4.38}{a_{siw}} e^{\frac{-0.627\varepsilon_r}{\varepsilon_e} \frac{\varepsilon_r + 1}{2} + \left(\frac{\varepsilon_r - 1}{2} \right) \left(1 + \frac{12h}{w} \right)^{-0.5}}$$

3. SLOTTED SIW ARRAY ANTENNA AT 28 GHZ

The slotted SIW array antenna is designed by shorting one side of the microstrip to SIW transition, and eight slots are etched in the longitudinal direction as depicted in Fig. 2. The slot length, the distance between two successive slots, and the distance from the last slot center to the center of the shorted via wall are calculated based on formulas discussed in paper [12]. When power is distributed uniformly, all slots are uniformly displaced from the longitudinal axis of the designed SIW array. As a result, they are excited equally in amplitude and phase. Uniform displacement (d_{equal}) is calculated from Equation (9). The SLL of the SIW array depends on the displacement of the slot as it varies the conductance with which the slot is excited. Slots are displaced so that they are excited based on the Chebyshev distribution to attain low SLL. Nonuniform Chebyshev displacements (d_n) are calculated from Equation (10), and these values are tabulated in Table 2. A Matlab programme has been written to generate the slot displacements for a desired SLL. Program inputs include design frequency, SIW dimensions a_{SIW} , substrate height, number of slots, and the highest allowed SLL.

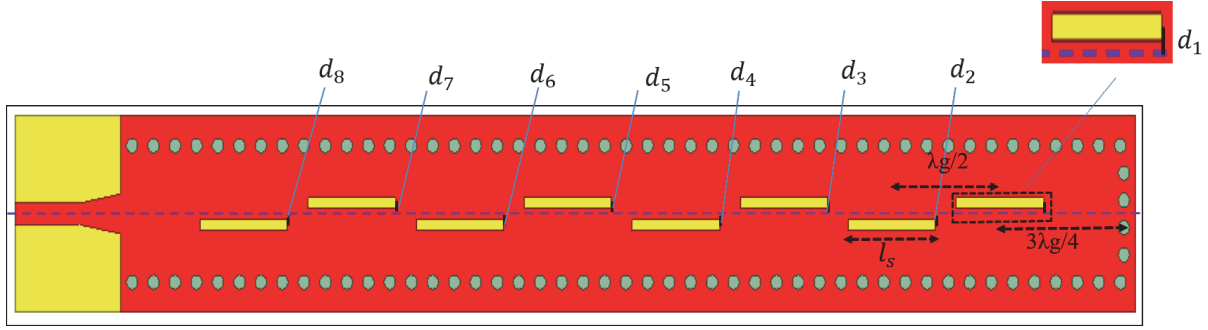


Figure 2. 1 × 8 Slotted SIW array.

Table 2. Dimensions of the slot displacements.

Slot displacement	Value (mm)	Slot displacement	value (mm)
d_1	0.126	d_6	0.289
d_2	0.214	d_7	0.214
d_3	0.289	d_8	0.126
d_4	0.332	d_{equal}	0.29
d_5	0.332		

The approximate equations for slot length (l_s) and width (w_s) are given by

$$\begin{aligned} \text{slot width } (w_s) &= \frac{\lambda_g}{20} \\ \text{slot length } (l_s) &= \frac{\lambda_0}{2\sqrt{\epsilon_r + 1}} \end{aligned} \quad (9)$$

$$d_{equal} = \frac{a_{SIW}}{\pi} \sqrt{\sin^{-1} \left[\frac{1}{N \times G} \right]}$$

where

$$\begin{aligned} G &= 2.09 \times \frac{a_{SIW}}{h} \times \frac{\lambda_g}{\lambda_0} \times \left[\cos \left(0.464\pi \times \frac{\lambda_0}{\lambda_g} \right) - \cos(0.464\pi) \right]^2 \\ d_n &= \frac{a_{SIW}}{\pi} \arcsin \sqrt{\frac{g_n}{2.09 \frac{\lambda_g}{\lambda_0} \frac{a_{SIW}}{h} \cos^2 \left(\frac{\pi \lambda_0}{2\lambda_g} \right)}} \end{aligned} \quad (10)$$

where

$$g_n = \frac{c_n}{\sum_{n=1}^N c_n}$$

where c_n 's are the Chebyshev coefficients for the desired SLL, and N is the number of slots.

4. EXPERIMENTAL RESULTS AND DISCUSSION

In order to verify the results, a prototype of the low SLL 1×8 SIW array was fabricated on an RT duriod5880 substrate whose dielectric constant is 2.2, and the thickness is 10 mil (0.254 mm) as shown in Fig. 3. A 2.92 mm SMA connector supported assembly was used with the fabricated antennas, which were tested using a PNA-X N5244B network analyzer (10 MHz–43.5 GHz) and pattern measurements performed in anechoic chamber as shown in Figs. 4(a) & (b). The measured $|S_{11}|$ is better than -10 dB at 28 GHz and compared with the simulation $|S_{11}|$ as shown in Fig. 5. Surface current distribution and 3D radiation pattern of a nonuniform 1×8 slotted SIW are shown in Fig. 6. Fig. 7 depicts the normalized co- and cross-pol radiation patterns of a uniform and nonuniform (Chebyshev) 1×8 SIW array and good acceptance between co- and cross-pol levels. Measured SLL of nonuniform 1×8 SIW

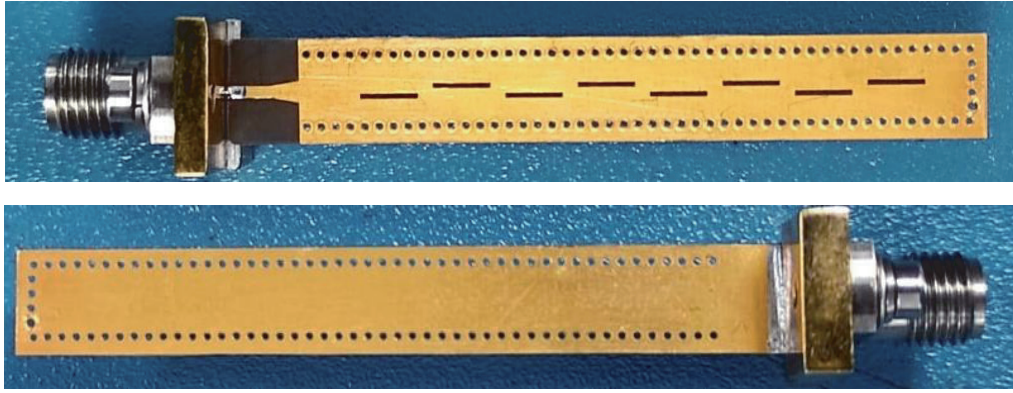


Figure 3. Top and bottom view fabricated 1×8 Slotted SIW array.

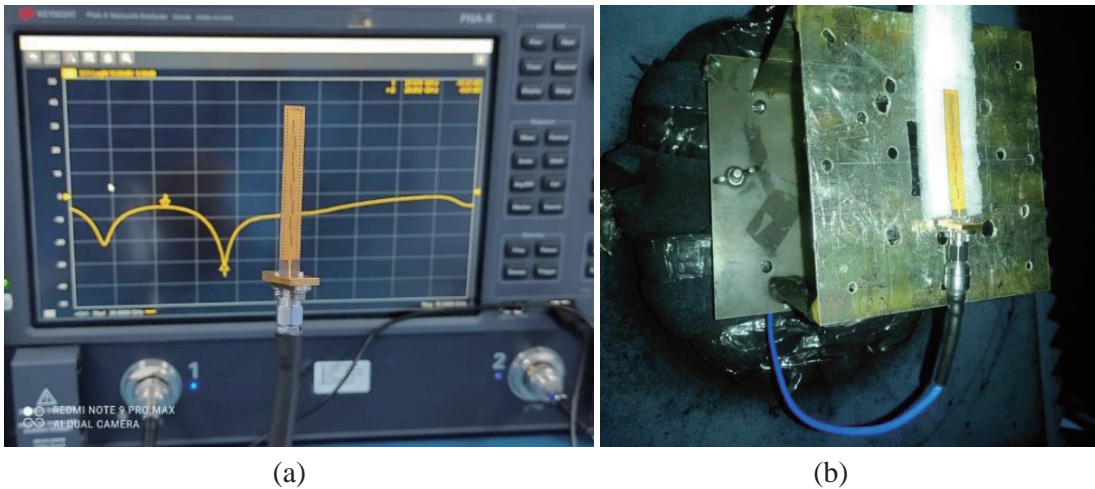


Figure 4. Photograph of measurement test setup of fabricated 1×8 SIW array with (a) PNA-X N5244B network analyzer, (b) Anechoic chamber.

array is -22 dB, which is -9 dB less than uniform distribution as shown in Fig. 8. Measured HPBW and gain are 17° and 13 dB, respectively, whereas HPBW and gain of uniform distribution are 14° and 14 dB.

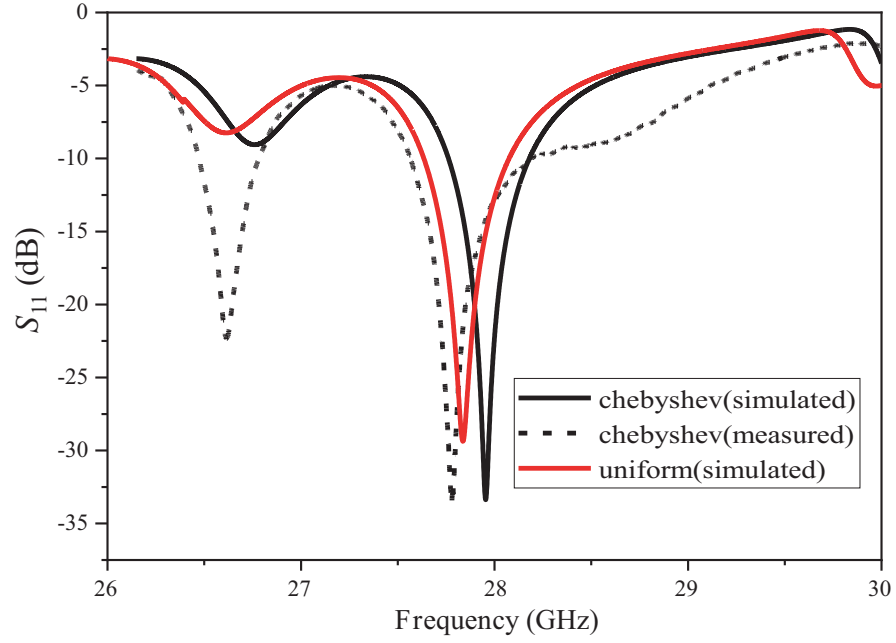
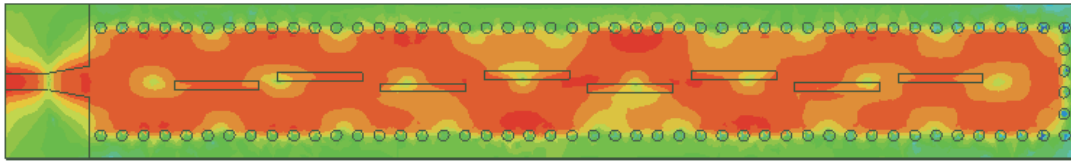
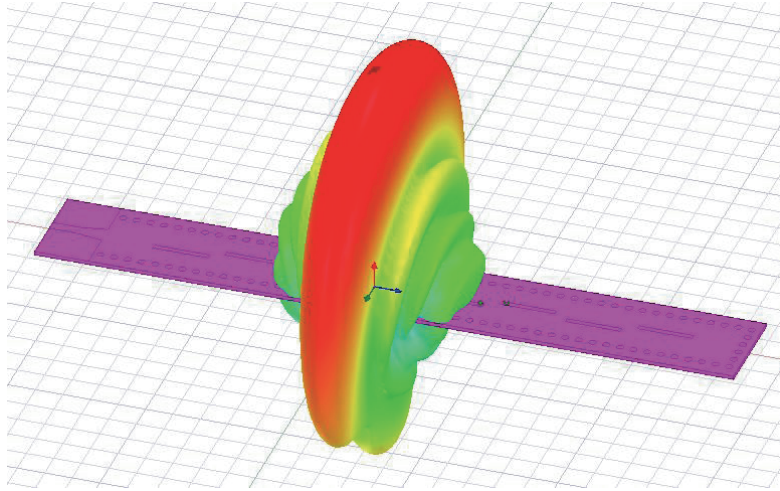


Figure 5. Reflection parameter of 1×8 slotted SIW array.



(a)



(b)

Figure 6. (a) Surface current distribution. (b) 3D radiation pattern of non-uniform 1×8 slotted SIW.

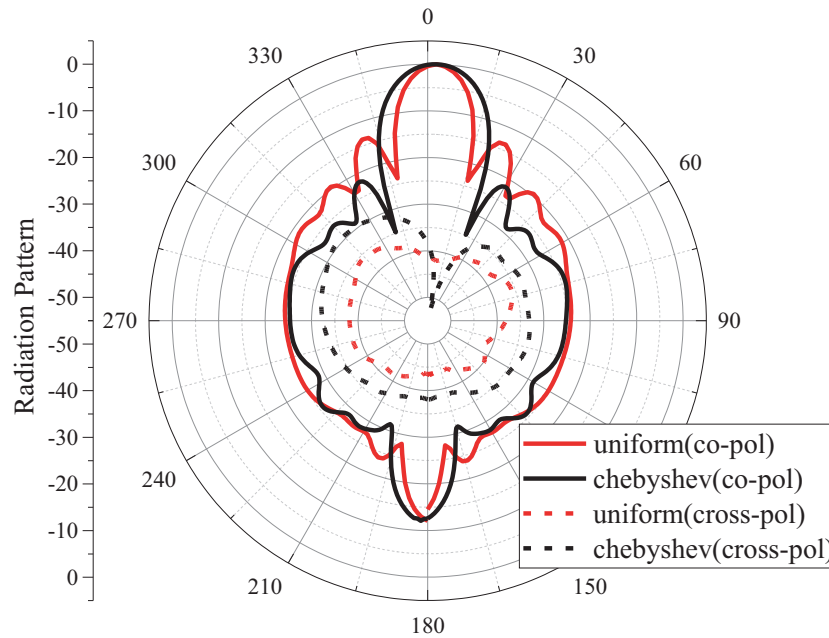


Figure 7. Simulated co and cross-pol radiation pattern of 1×8 slotted SIW array.

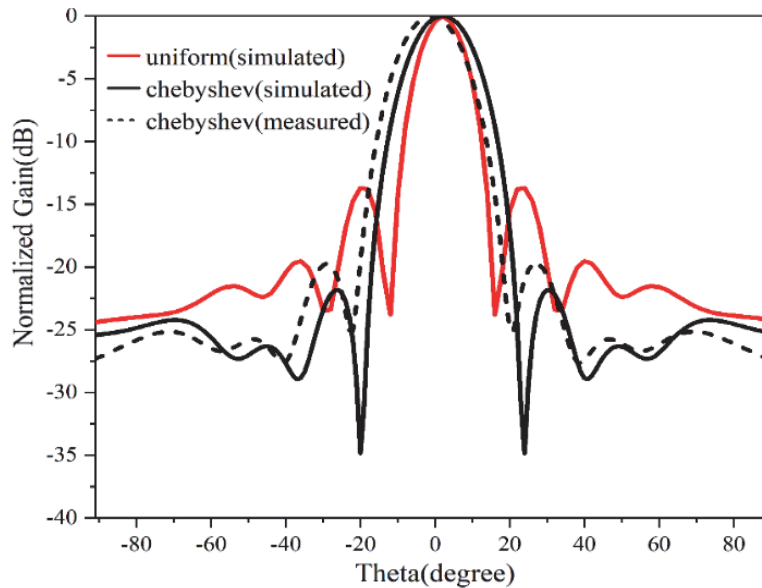


Figure 8. Simulated vs measured pattern of 1×8 SIW array.

Finally, the measured and simulated gains, SLLs, and beamwidths of the slotted SIW array at 28 GHz are summarized, as listed in Table 3. According to Table 3, there is a 0.1 dB variation in the gain, a 1 dB variation in the SLL, and a 1° variation in the beamwidth in the measured and simulation values. The connector losses and measurement uncertainties may account for the variation.

Table 4 summarises the designed slotted SIW array compared with previous reported works in the literature. Moreover, in this work Chebyshev distribution is used to find the displacements of the slots in the 1×8 SIW array to get optimum SLL. A reduction in SLL of -9 dB was achieved in comparison to the uniform SIW slotted array antenna. The present work has a low SLL compared with the other techniques

Table 3. Antenna performance results.

Antenna Parameter	uniform distribution (simulated)	Chebyshev distribution (simulated)	Chebyshev distribution (measured)
Return loss	29 dB	33 dB	33 dB
Bandwidth	500 MHz	550 MHz	550 MHz
Peak gain (dB)	14	13	12.9
SLL (dB)	−13.85	−22	−21
Beamwidth	13°	18°	17°

Table 4. Comparison with previous works.

Ref. No.	Frequency (GHz)	Number of slots	Gain (dB)	SLL (dB)	Technique	Size (mm ³)
[13]	94	1 × 12	9.2	−28	amplitude tapering by changing the SIW width	0.41λ _o ³
[14]	24	32 × 4	22.8	−20	Taylor distribution	3.35λ _o ³
[15]	10	16 × 16	24	−30	Taylor continuous distribution root matching sampling	3.9λ _o ³
[16]	28	1 × 8	13	−20	Taylor distribution with unequal feeding network	9.2λ _o ³
This work	28	1 × 8	13	−22	Chebyshev distribution	0.076λ _o ³

provided in [14, 16]. Although some of the works have low SLL, the gain is less even with more slots in [13], and the complexity is greater in terms of structure and the feeding network in [15, 16]. It is clearly observed that the designed antenna has a smaller footprint ($0.667\lambda_o \times 4.84\lambda_o \times 0.023\lambda_o = 0.0766\lambda_o^3 \text{ mm}^3$) along with good gain, low SLL, and low cross polarization which makes this antenna suitable for radar and wireless applications.

5. CONCLUSION

The low SLL and optimum gain 1 × 8 slotted SIW array antenna at 28 GHz was presented. The antenna prototype was fabricated, tested, and the measurements were compared to simulation data. A −22 dB SLL is achieved by applying Chebyshev coefficients in the form of displacement of the slot with respect to the longitudinal axis of the SIW. The presented antenna has a gain of 13.5 dB, a low side lobe level of −22 dB, and a greater than 30 dB cross polarization level, which makes this antenna suitable for radar and wireless applications.

ACKNOWLEDGMENT

This research was carried out at the “Centre for Excellence in Microwave Engineering Laboratory,” Department of ECE, Osmania University, Hyderabad, Telangana, India.

REFERENCES

1. Huang, G.-L., S.-G. Zhou, T.-H. Chio, H.-T. Hui, and T.-S. Yeo, "A low profile and low sidelobe wideband slot antenna array fed by an amplitude-tapering waveguide feed-network," *IEEE Transactions on Antennas and Propagation*, Vol. 63, No. 1, 419–423, Jan. 2015.
2. Deslandes, D. and K. Wu, "Integrated microstrip and rectangular waveguide in planar form," *IEEE Microwave and Wireless Components Letters*, Vol. 11, No. 2, 68–70, Feb. 2001.
3. Yan, L., W. Hong, K. Wu, and T. J. Cui, "Investigations on the propagation characteristics of the substrate integrated waveguide based on the method of lines," *IEE Proceedings — Microwaves, Antennas and Propagation*, Vol. 152, No. 1, 35–42, Feb. 19, 2005.
4. Xu, F. and K. Wu, "Numerical multimode calibration technique for extraction of complex propagation constants of substrate integrated waveguide," *2004 IEEE MTT-S International Microwave Symposium Digest (IEEE Cat. No. 04CH37535)*, Vol. 2, 1229–1232, Fort Worth, TX, USA, 2004.
5. Xu, F., Y. Zhang, W. Hong, K. Wu, and T. J. Cui, "Finite-difference frequency-domain algorithm for modeling guided-wave properties of substrate integrated waveguide," *IEEE Transactions on Microwave Theory and Techniques*, Vol. 51, No. 11, 2221–2227, Nov. 2003.
6. Cassivi, Y., L. Perregrini, P. Arcioni, M. Bressan, K. Wu, and G. Conciauro, "Dispersion characteristics of substrate integrated rectangular waveguide," *IEEE Microwave and Wireless Components Letters*, Vol. 12, No. 9, 333–335, Sept. 2002.
7. Kunooru, B., S. V. Nandigama, D. Rama Krishna, R. Gugulothu, and S. Bhalke, "Studies on microstrip to SIW transition at Ka-Band," *2019 TEQIP III Sponsored International Conference on Microwave Integrated Circuits, Photonics and Wireless Networks (IMICPW)*, 379–382, 2019.
8. Deslandes, D., "Design equations for tapered microstrip-to-Substrate Integrated Waveguide transitions," *2010 IEEE MTT-S International Microwave Symposium*, 704–707, 2010.
9. Bozzi, M., A. Georgiadis, and K. Wu, "Review of substrate-integrated waveguide circuits and antennas," *IET Microwaves, Antennas Propagation*, Vol. 5, No. 8, 909–920, Jun. 2011.
10. Stevenson, A. F., "Theory of slots in rectangular waveguides," *Journal of Applied Physics*, Vol. 19, 24–38, 1948.
11. Elliott, R., "On the design of traveling-wave-fed longitudinal shunt slot arrays," *IEEE Transactions on Antennas and Propagation*, Vol. 27, No. 5, 717–720, Sept. 1979.
12. El Misilmani, H. M., M. Al-Husseini, and M. Mervat, "Design of slotted waveguide antennas with low sidelobes for high power microwave applications," *Progress In Electromagnetics Research C*, Vol. 56, 15–28, 2015.
13. Dewantari, A., J. Kim, I. Scherbatko, and M.-H. Ka, "A sidelobe level reduction method for mm-wave substrate integrated waveguide slot array antenna," *IEEE Antennas and Wireless Propagation Letters*, Vol. 18, No. 8, 1557–1561, Aug. 2019.
14. Xu, J., Z. N. Chen, and X. Qing, "CPW center-fed single-layer SIW slot antenna array for automotive radars," *IEEE Transactions on Antennas and Propagation*, Vol. 62, No. 9, 4528–4536, Sept. 2014.
15. Xu, J. F., W. Hong, P. Chen, and K. Wu, "Design and implementation of low sidelobe substrate integrated waveguide longitudinal slot array antennas," *IET Microw., Antennas Propag.*, Vol. 3, No. 5, 790–797, 2009.
16. Park, S., D. Shin, and S. Park, "Low side-lobe substrate-integrated-waveguide antenna array using broadband unequal feeding network for millimeter-wave handset device," *IEEE Transactions on Antennas and Propagation*, Vol. 64, No. 3, 923–932, Mar. 2016.
17. Zong, Y., J. Ding, C.-J. Guo, and C. Li, "A novel center-fed SIW inclined slot antenna for active phased array," *Progress In Electromagnetics Research Letters*, Vol. 88, 97–104, 2020.